

On the Interference Robustness of Ultra-Wideband Energy Detection Receivers

Christoph Steiner and Armin Wittneben

Communication Technology Laboratory, Swiss Federal Institute of Technology (ETH) Zurich

Email: {steinech,wittneben}@nari.ee.ethz.ch

Abstract—This work analyzes the performance of Ultra-Wideband energy detection receivers for binary pulse position modulation in the presence of narrowband or wideband interference. The decision variable after the integrator of an energy detector is separated into a signal and an interference term. An analytical expression for the variance of the interference term is derived. This variance indicates the detection performance and is minimized by choosing optimal values for the integration time of the energy detection receiver. Fundamental performance limits of energy detection receivers in case of wideband interference are found and discussed. A linear pulse correlation receiver is considered for reference performance results.

I. INTRODUCTION

Ultra-Wideband (UWB) is foreseen to be the key technology for developing ultra low-power communication systems [1]. The transmit power of UWB systems is limited by regulatory authorities worldwide such as the Federal Communications Commission (FCC) [2] in the United States and the Electronic Communications Committee (ECC) [3] in Europe. The main goal is to ensure negligible interference of UWB devices to existing systems, but also the overall power consumption of UWB transmitter is reduced by this constraint. Moreover, UWB technology enables very low complexity transceivers, especially if the UWB impulse radio paradigm in conjunction with pulse position modulation (PPM) and energy detection is applied. Such a low power transceiver structure with an estimated current consumption of 40 mA is presented in [4]. A similar design with even lower complexity and an estimated current consumption of less than 1 mA is presented in [5]. These low-power and low-complexity receiver realizations in [4] and [5] utilize a non-coherent energy detection approach.

However, a huge drawback of these receivers is their vulnerability to interference from other existing communication systems. The signal-to-interference ratio at the receive antenna can be up to -50 dB, if, for example, WLAN is considered as interferer in vicinity of the UWB receiver. In contrast to out-of-band interferers, the signal-to-interference ratio cannot be improved by filtering for in-band interferers. In this case, it depends on the receiver architecture, mitigation techniques, and the structure of the interference, whether bit detection is still possible. Out-of-band signals are attenuated by the transfer function of the UWB antenna and the band selection filter. Nevertheless, this attenuation depends on the filter order and could be too low for strong interferers. Furthermore, if the interference power at the input of the low noise amplifier is in the range of the signal power, intermodulation products

due to nonlinearities of the low noise amplifier can fall into the desired band. These intermodulation products cannot be filtered by subsequent bandpass filters and act as in-band interference.

Some work has been dedicated to the investigation of the impact of interference on UWB receivers. A performance analysis of a linear pulse correlation receiver in the presence of interference is given in [6]. Transmitted reference receiver performance in the presence of narrowband interference is treated in [7], [8] and a mitigation technique for differential transmitted reference receivers is presented in [9]. However, for the important case of a low complexity energy detection receiver no such analysis exists to the best of the authors' knowledge. Therefore, this work analyzes the impact of narrowband and wideband interference on the performance of PPM energy detection receivers.

In Section II, the signal model for binary PPM and the interference is presented. The signal-to-interference ratios for the pulse correlation receiver and the energy detector are derived in Sections III and IV, respectively. The performance of the receivers depending on system and interference parameters is evaluated in Section V. Finally, Section VI summarizes the work and gives conclusions.

II. SIGNAL MODEL

A single user UWB communication link is considered, where binary PPM is applied. The system performance is investigated in the presence of a strong interference source, such that the additional performance degradation due to thermal noise is negligible. The received signal is given as

$$r(t) = \sqrt{E_p} \sum_k p(t - kT_b - d_k T_b/2) + i(t), \quad (1)$$

where $i(t)$ is the interfering signal, and $p(t)$ is the UWB pulse waveform with energy one. The bit rate is $1/T_b$ and the length of a PPM slot is $T_b/2$. The data symbols $d_k \in \{0, 1\}$ are assumed statistically independent and equally probable. One pulse per bit is used and the transmit energy per bit is E_p . The following simplifying assumptions are made for the sake of analytical tractability:

- 1) The UWB pulse is modeled as

$$p(t) = \begin{cases} \sqrt{\frac{2}{T_p}} \cos(2\pi f_c t) & 0 < t < T_p \\ 0 & \text{otherwise,} \end{cases} \quad (2)$$

with $0 < T_p \leq T_b/2$. The energy of this pulse for arbitrary T_p and f_c is given by

$$\int_0^{T_p} p^2(t)dt = 1 + \frac{1}{4\pi f_c T_p} \sin(4\pi f_c T_p).$$

If the carrier frequency is large compared to the integration time, i.e., $4\pi f_c T_p \gg 1$, the sine term is negligible and the pulse energy reduces to one Joule.

- 2) The effect of the UWB multipath channel is not considered. Thus, the transmit pulse arrives at the receiver undistorted. Moreover, perfect synchronization is assumed.
- 3) The interfering signal $i(t)$ is modeled as a realization of a continuous-time, wide sense stationary, zero mean Gaussian process $I(t)$ with center frequency f_I , bandwidth W_I and autocorrelation function

$$R_I(\tau) = P_I \frac{\sin(\pi W_I \tau)}{\pi W_I \tau} \cos(2\pi f_I \tau),$$

where P_I is the power of the interferer.

The signal-to-interference ratio at the input of the receiver is defined as

$$\text{SIR}_{\text{in}} = 10 \log_{10} \left(\frac{P_s}{P_I} \right) = 10 \log_{10} \left(\frac{E_p}{T_b P_I} \right),$$

where the signal power is given as $P_s = E_p/T_b$.

According to the modeling assumptions each data symbol d_k can be treated separately. Therefore, k is set to zero in the following considerations.

III. PULSE CORRELATION RECEIVER

The receiver, which optimizes the signal-to-noise ratio in case of additive white Gaussian noise, is the pulse correlation receiver or, equivalently, the matched filter receiver. It performs a correlation of the received signal $r(t)$ with the template waveform

$$v(t) = p(t) - p(t - T_b/2).$$

The correlator output corresponding to information bit d_0 is given for $4\pi f_c T_p \gg 1$ according to [6] as

$$Y_{\text{cr}} = \int_0^{T_b} r(t)v(t)dt = \pm \sqrt{E_p} + I_{\text{cr}},$$

where the random variable I_{cr} is a filtered zero mean Gaussian process and therefore Gaussian distributed. Consequently, the variance of I_{cr} determines the detection performance and the signal-to-interference ratio of the decision variable of the correlation receiver is defined as

$$\text{SIR}_{\text{cr}} = 10 \log_{10} \left(\frac{E_p}{\text{E}\{I_{\text{cr}}^2\}} \right),$$

where $\text{E}\{I_{\text{cr}}^2\}$ denotes the expected value of the random variable I_{cr}^2 , i.e., the variance of I_{cr} . Applying similar steps

as in [6] and considering the different pulse shape $p(t)$, the expectation is given by

$$\text{E}\{I_{\text{cr}}^2\} = \frac{2}{T_p} \int_0^{T_p} \int_0^{T_p} \left\{ \cos(2\pi f_c(t_1 + t_2)) - \cos(2\pi f_c(t_1 - t_2)) \right\} R_I(t_1 - t_2) dt_1 dt_2 \quad (3)$$

$$- \frac{2}{T_p} \int_0^{T_p} \int_0^{T_p} \left\{ \cos(2\pi f_c(t_1 + t_2)) - \cos(2\pi f_c(t_1 - t_2)) \right\} R_I\left(t_1 - t_2 - \frac{T_b}{2}\right) dt_1 dt_2. \quad (4)$$

The shift of $T_b/2$ in the autocorrelation function in conjunction with the bandwidth of the interferer W_I determines the similarity of (3) and (4), and consequently the variance of I_{cr} . Furthermore, the integration interval T_p in conjunction with f_c and f_I shows significant impact on this variance. These effects are discussed in Section V.

IV. ENERGY DETECTION RECEIVER

The energy detection receiver computes

$$Y_{\text{ed}} = \int_0^{T_p} r(t)^2 dt - \int_{T_b/2}^{T_b/2+T_p} r(t)^2 dt = s + I_{\text{ed}},$$

where s accounts for the signal part and I_{ed} for the interference part. For the pulse shape defined in (2), s is given by

$$s = \begin{cases} E_p \left(1 + \frac{1}{4\pi f_c T_p} \sin(4\pi f_c T_p) \right), & d_0 = 0 \\ -E_p \left(1 + \frac{1}{4\pi f_c T_p} \sin(4\pi f_c T_p) \right), & d_0 = 1. \end{cases}$$

If the carrier frequency is large compared to the integration time, i.e., $4\pi f_c T_p \gg 1$, the sine terms are negligible and the signal sample reduces to $s = \pm E_p$.

Due to the squaring operation, the interfering sample $I_{\text{ed}} = I_1 + I_2 + I_3$ consists of the three summands given below:

$$I_1 = 2\sqrt{\frac{2E_p}{T_p}} \begin{cases} \int_0^{T_p} \cos(2\pi f_c t) I(t) dt, & d_0 = 0 \\ -\int_0^{T_p} \cos(2\pi f_c t) I(t + T_b/2) dt, & d_0 = 1 \end{cases} \quad (5)$$

$$I_2 = \int_0^{T_p} I^2(t) dt, \quad (6)$$

$$I_3 = -\int_{T_b/2}^{T_b/2+T_p} I^2(t) dt. \quad (7)$$

The first term (5) contains the mixed signal-interference components of Y_{ed} , i.e., it depends on the interference as well as on the signal. The other interfering terms (6) and (7) are independent of the transmitted signal.

Since $I(t)$ is modeled as zero mean wide sense stationary, it follows that $\text{E}\{I_{\text{ed}}\} = 0$. However, I_{ed} is not Gaussian distributed due to terms (6) and (7). Nevertheless, the variance of I_{ed} is assumed to be a detection performance indicator, because a smaller variance implies a lower detection error probability. Therefore, the signal-to-interference ratio of the

decision variable for the energy detection receiver is defined as

$$\text{SIR}_{\text{ed}} = 10 \log_{10} \left(\frac{E_p^2}{\text{E}\{I_{\text{ed}}^2\}} \right).$$

The variance of I_{ed} for $d_0 = 0$ is given by

$$\text{E}\{I_{\text{ed}}^2 | d_0 = 0\} = \frac{8E_p}{T_p} \int_0^{T_p} \int_0^{T_p} \cos(2\pi f_c t_1) \cos(2\pi f_c t_2) \times \text{E}\{I(t_1)I(t_2)\} dt_1 dt_2 \quad (8)$$

$$+ \sqrt{\frac{8E_p}{T_p}} \int_0^{T_p} \int_0^{T_p} \cos(2\pi f_c t_1) \text{E}\{I(t_1)I^2(t_2)\} dt_1 dt_2 \quad (9)$$

$$- \sqrt{\frac{8E_p}{T_p}} \int_0^{T_p} \int_{T_b/2}^{T_b/2+T_p} \cos(2\pi f_c t_1) \text{E}\{I(t_1)I^2(t_2)\} dt_1 dt_2 \quad (10)$$

$$+ 2 \int_0^{T_p} \int_0^{T_p} \text{E}\{I^2(t_1)I^2(t_2)\} dt_1 dt_2 \quad (11)$$

$$- 2 \int_0^{T_p} \int_{T_b/2}^{T_b/2+T_p} \text{E}\{I^2(t_1)I^2(t_2)\} dt_1 dt_2. \quad (12)$$

The variance of I_{ed} for $d_0 = 1$ remains unchanged due to the stationarity of the interference. The expected values for the summands (9) and (10) are zero, since $\text{E}\{X_1 X_2^2\} = 0$ for a zero mean random variable X_1 .

The expected values in (11) and (12) can be expressed in terms of the autocorrelation function $\text{E}\{I(t_1)I(t_2)\} = R_I(t_1 - t_2)$ according to $\text{E}\{I^2(t_1)I^2(t_2)\} = R_I^2(0) + 2R_I^2(t_1 - t_2)$. This is derived in [10], where the expected values $\text{E}\{X_1^2 X_2^2\}$ for $X_1 = I(t_1)$ and $X_2 = I(t_2)$ are computed. Therefore, the variance of the interfering sample is given by

$$\begin{aligned} \text{E}\{I_{\text{ed}}^2\} &= \frac{4E_p}{T_p} \int_0^{T_p} \int_0^{T_p} \left\{ \cos(2\pi f_c(t_1 + t_2)) \right. \\ &\quad \left. - \cos(2\pi f_c(t_1 - t_2)) \right\} R_I(t_1 - t_2) dt_1 dt_2 \\ &+ 4 \int_0^{T_p} \int_0^{T_p} R_I^2(t_1 - t_2) dt_1 dt_2 \\ &- 4 \int_0^{T_p} \int_{T_b/2}^{T_b/2+T_p} R_I^2(t_1 - t_2) dt_1 dt_2. \end{aligned}$$

The double integrals can be reduced to a single integral by substituting $\tau = t_1 - t_2$, which gives

$$\begin{aligned} \text{E}\{I_{\text{ed}}^2\} &= \frac{8E_p}{T_p} \left(\int_0^{T_p} (T_p - \tau) R_I(\tau) \cos(2\pi f_c \tau) d\tau \right. \\ &\quad \left. + \frac{1}{4\pi f_c} \int_0^{T_p} R_I(\tau) \left(\sin(2\pi f_c(2T_p - \tau)) - \sin(2\pi f_c \tau) \right) d\tau \right) \quad (13) \end{aligned}$$

$$+ 8 \int_0^{T_p} (T_p - \tau) R_I^2(\tau) d\tau \quad (14)$$

$$- 4 \int_{-T_p}^{T_p} (T_p - |\tau|) R_I^2\left(\tau + \frac{T_b}{2}\right) d\tau. \quad (15)$$

The first term (13) accounts for the mixed product of the UWB pulse and interfering signal. Its value strongly depends on the parameters T_p , f_c , and f_I . These dependencies are investigated in Section V. It can be seen from (3) that the derivation of $\text{E}\{I_{\text{cr}}^2\}$ for the pulse correlation receiver yields a similar expressions as (13), whereas the term (4) is not present in $\text{E}\{I_{\text{ed}}^2\}$.

The last two terms (14) and (15) are only due to the interfering signal. These terms do not appear in the expression for the variance of the interference for the pulse correlation receiver. Since energy detection subtracts the energy in the second PPM slot from the energy in the first one, (15) is subtracted from (14). Therefore, the variance reduction due to (15) depends mainly on the temporal separation $T_b/2$ and the bandwidth W_I of the interfering signal.

V. PERFORMANCE ANALYSIS

This section analyzes the expressions for the variance of the interference part of the decision variable in case of narrowband interference ($W_I \ll 1/T_p$) and wideband interference ($W_I \rightarrow 1/T_p$). Furthermore, results for the signal-to-interference ratio of the decision variable of energy detection and pulse correlation receiver are presented and discussed.

A. Narrowband Interference

If the bandwidth of the interfering signal is negligible compared to the bandwidth of the UWB signal, i.e., $W_I \ll 1/T_p$, the autocorrelation function of the narrowband interfering signal can be approximated with

$$R_{I,nb}(\tau) = P_I \cos(2\pi f_I \tau).$$

The expression for the variance of I_{ed} reduces to the two functions $F_{1,nb}$ accounting for (13) and $F_{2,nb}$ accounting for (14) and (15) according to

$$\text{E}\{I_{\text{ed}}^2\} = F_{1,nb} + F_{2,nb}, \text{ with}$$

$$\begin{aligned} F_{1,nb}(E_p, T_p, f_c, f_I, P_I) &= \frac{E_p P_I}{T_p \pi^2 (f_c^2 - f_I^2)^2} \left\{ f_c^2 + 3f_I^2 \right. \\ &\quad \left. + (f_I^2 - f_c^2) \cos(4\pi f_c T_p) - 2f_I(f_c + f_I) \cos(2\pi(f_c - f_I)T_p) \right. \\ &\quad \left. - 2f_I^2 \cos(2\pi(f_c + f_I)T_p) + 2f_c f_I \cos(2\pi(f_c + f_I)T_p) \right\}, \quad (16) \end{aligned}$$

$$\begin{aligned} F_{2,nb}(T_p, T_b, f_I, P_I) &= \frac{P_I^2}{8\pi^2 f_I^2} \\ &\quad \left\{ 2 - 2\cos(2\pi f_I T_b) + \cos(2\pi f_I (T_b - 2T_p)) \right. \\ &\quad \left. - 2\cos(4\pi f_I T_p) + \cos(2\pi f_I (T_b + 2T_p)) \right\}. \quad (17) \end{aligned}$$

The carrier frequency f_c and the integration time (pulse width) T_p are the adjustable parameters of the UWB communication system. Therefore, these parameters should be adapted according to (16) and (17), such that the variance of the interference sample I_{ed} becomes minimal. It is not practical to adapt f_c to the possibly varying interference, since all analog hardware components like filters and amplifiers are designed for a specific f_c . On the other hand, it is quite easy to adapt T_p ,

since only the integrator block is affected. If the integration of the squared receive signal is realized by a low pass filter as in [5], the adaption of T_p would correspond to a change of the filter bandwidth, which is easy to implement. Thus, optimization of T_p is considered in the following.

The following parameter values are used throughout the remaining paper. The interference power is set to the signal power $P_I = P_s$, which implies an SIR_{in} of 0 dB. The carrier frequency of the UWB pulse is $f_c = 3.75$ GHz, and the bit period T_b is 20 ns. In order to find the optimal values of T_p for given E_p , P_I , f_I , f_c , and T_b , the partial derivatives with respect to T_p of $F_{1,nb}$ and $F_{2,nb}$ must be calculated and equated to zero. These equations are transcendental, meaning that no closed-form solution can be provided. However, for visual inspection snapshots of the functions $F_{1,nb}$ and $F_{2,nb}$ for varying T_p and f_I are depicted in Fig. 1 and Fig. 2, respectively, where the values of $F_{1,nb}$ and $F_{2,nb}$ are normalized to E_p^2 .

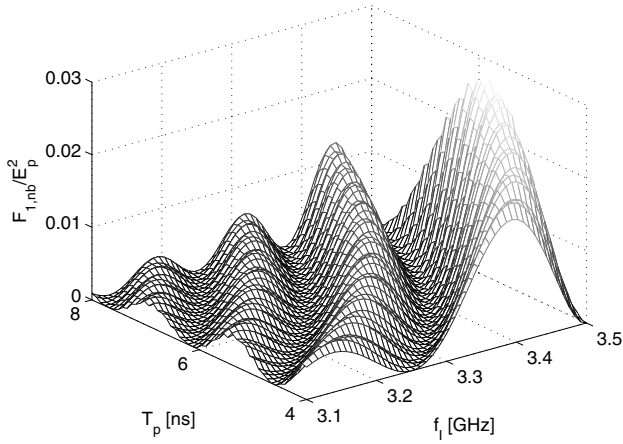


Fig. 1. First part of the variance of I_{ed}

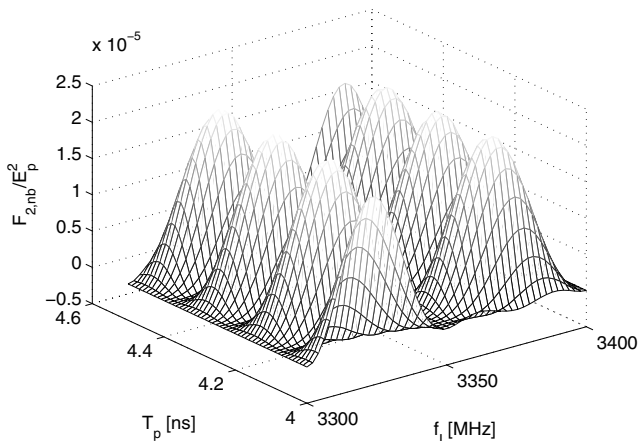


Fig. 2. Second part of the variance of I_{ed}

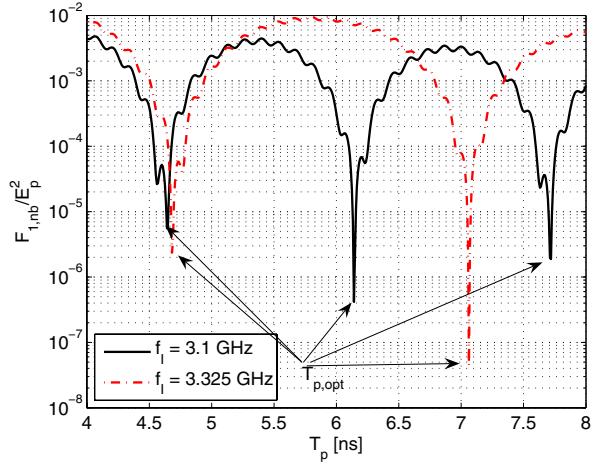


Fig. 3. First part of the variance of I_{ed} for fixed f_I and varying T_p

It can be seen from (17) and Fig. 2 that $0 \leq F_{2,nb} \leq \frac{P_I^2}{\pi^2 f_I^2}$. If the cosine terms in (17) cancel each other, the lower bound is achieved. On the other hand, if they add up coherently, the upper bound is achieved. The upper bound decreases with increasing f_I , because more full periods of the interfering signal fall into one PPM slot implying more similar interference energy in two subsequent PPM slots and, consequently, an increased interference suppression by subtracting the second PPM from the first PPM slot. It can also be seen that the maximum value of $F_{2,nb}$ is order of magnitudes smaller than the maximum value of $F_{1,nb}$ due to the narrowband nature of the interference. Therefore, at first only $F_{1,nb}$ is considered, in order to find optimum values for T_p , such that the variance of the interfering sample I_{ed} is minimal. Fig. 3 depicts cuts at $f_I = 3.1$ GHz and $f_I = 3.325$ GHz of $F_{1,nb}$. It can be read from Fig. 3 that there are minimum values of $F_{1,nb}$ for T_p at

$$T_{p,\text{opt}} \approx \{4.6, 6.2, 7.7\} \text{ ns for } f_I = 3.1 \text{ GHz}$$

$$T_{p,\text{opt}} \approx \{4.7, 7.1\} \text{ ns for } f_I = 3.325 \text{ GHz,}$$

which corresponds to the general condition

$$T_{p,\text{opt}} = \frac{k}{|f_c - f_I|} \text{ for } k \in \{1, 2, \dots\}. \quad (18)$$

If T_p is chosen according to condition (18), the values for $F_{1,nb}$ are bounded by

$$0 \leq F_{1,nb} \leq \frac{2E_p P_I |f_c - f_I|}{k\pi^2 (f_c + f_I)^2},$$

where the lower bound is achieved for $\cos(4\pi f_c T_p) = \cos(2\pi(f_c + f_I)T_p) = 1$ and the upper bound is achieved for $\cos(4\pi f_c T_p) = \cos(2\pi(f_c + f_I)T_p) = -1$. The aforementioned bounds for $F_{2,nb}$ are still valid.

Fig. 4 depicts the two terms $F_{1,nb}$ and $F_{2,nb}$ for increasing f_I and $T_p = \frac{1}{|f_c - f_I|}$. It is observed from Fig. 4 that $F_{1,nb}/E_p^2 < 10^{-3}$ and $F_{2,nb}/E_p^2 < 10^{-4}$, implying an $\text{SIR}_{\text{ed}} > 29.5$ dB and efficient narrowband interference suppression. Furthermore, the values for $F_{1,nb}$ approach zero for

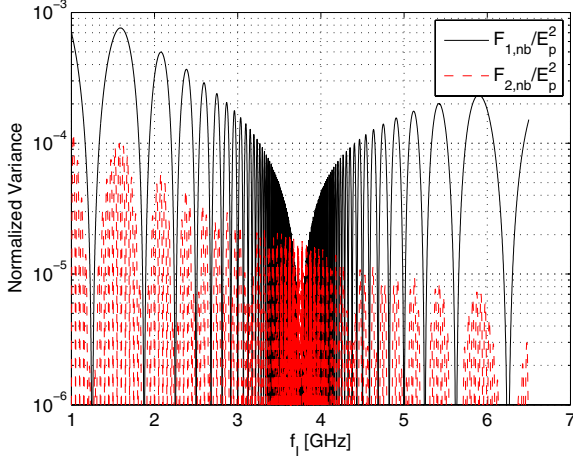


Fig. 4. Variance of I_{ed} for $T_p = \frac{1}{|f_c - f_I|}$

$f_I \rightarrow f_c$, which is in accordance to (16). Consequently, $F_{2,nb}$ starts to dominate the overall variance. However, the normalized values are smaller than 10^{-4} ($\text{SIR}_{ed} > 40$ dB), which implies that the more critical inband interference can be suppressed more efficiently, than interference with large $|f_I - f_c|$.

Condition (18) implies in the Fourier domain that f_I lies exactly at zeros of the sinc spectrum of the UWB pulse (2). This explains the vanishing variance for the linear interference part of the energy detection receiver ($F_{1,nb}$) for narrowband interference. Furthermore, the variance expression for the correlation receiver looks similar to the linear part of the energy detection receiver and experiences the same vanishing effect, if condition (18) holds. However, since no quadratic interference terms are present for the correlation receiver, this effect is also present for wideband interference, whereas it diminishes for the energy detection receiver, because the quadratic interference part ($F_{2,nb}$) starts to dominate the overall variance.

It can be concluded that the variance of the interference sample I_{ed} reaches local minima in case of narrowband interference, if the integration time T_p is set to values in accordance to (18). Thus, in order to optimize the signal-to-interference ratio of the energy detection receiver, only the carrier frequency of the interferer must be known or estimated.

B. Wideband Interference

If the interference becomes wideband, the increasing difference between terms (14) and (15) starts to dominate the variance of I_{ed} . Since the wideband autocorrelation function includes the sinc term, no closed form expressions of the integrals can be provided. However, equations (13), (14), and (15) are used to calculate $F_{1,wb}$ and $F_{2,wb}$. The function $F_{1,wb}$ accounts for the mixed product between signal and interference (13), and the function $F_{2,wb}$ accounts for the quadratic interference terms (14) and (15).

Fig. 5 shows values for $F_{1,wb}$ and $F_{2,wb}$ for increas-

ing T_p accounting for the wideband expressions of (13), (14), and (15), respectively. The bandwidth of the interference W_I is set to 1 MHz and 100 MHz. Fig. 6 depicts the two functions $F_{1,wb}$ and $F_{2,wb}$ for increasing W_I and $T_p = \frac{2}{|f_c - f_I|} \approx 4.7$ ns. The carrier frequency of the interferer is set to $f_I = 3.325$ GHz in both figures.

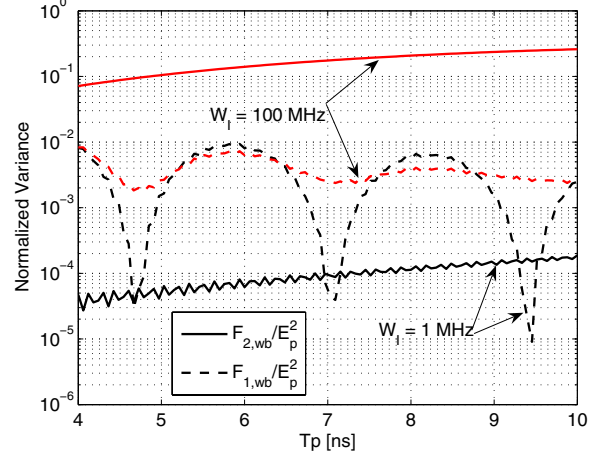


Fig. 5. Variance of I_{ed} for varying integration times T_p

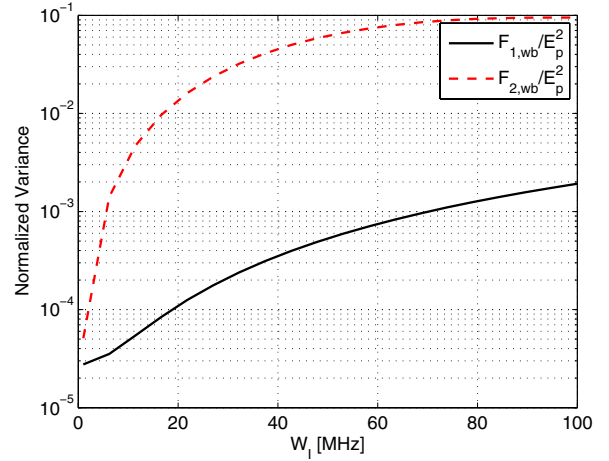


Fig. 6. Variance of I_{ed} for increasing bandwidths W_I

Fig. 5 and Fig. 6 show that the term $F_{2,wb}$ starts to dominate the overall variance. But also the minimum values for $F_{1,wb}$, which are still at T_p fulfilling condition (18), increase with increasing bandwidth.

The difference of the signal-to-interference ratios at the receiver input SIR_{in} and the decision variables SIR_{ed} and SIR_{cr} in dB determines the interference suppression capability of the respective receivers, which is also called processing gain (PG).

$$\text{PG}_{ed} = \text{SIR}_{ed} - \text{SIR}_{in} = 10 \log_{10} \left(\frac{E_p T_b P_I}{\mathbb{E} \{ I_{ed}^2 \}} \right),$$

$$\text{PG}_{cr} = \text{SIR}_{cr} - \text{SIR}_{in} = 10 \log_{10} \left(\frac{T_b P_I}{\mathbb{E} \{ I_{cr}^2 \}} \right).$$

It is apparent from the definitions for SIR_{in} and SIR_{ed} that the PG_{ed} for the energy detection receiver also depends on E_p . Thus, for a higher SIR_{in} , a higher PG_{ed} can be expected.

Fig. 7 depicts the PGs as function of T_p for the correlation receiver and the energy detection receiver for $f_I = 3.325$ GHz and $W_I \in \{1, 10, 100\}$ MHz. The PG for the correlation receiver does not change significantly, when changing W_I from 1 MHz to 10 MHz. Therefore, this curve is not shown in Fig. 7.

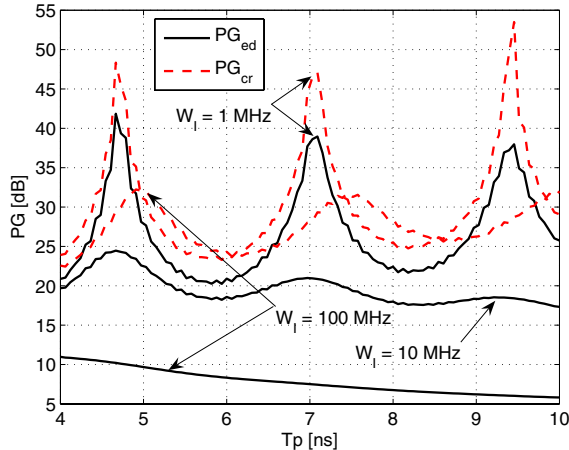


Fig. 7. Processing gains for correlation receiver and energy detection receiver for increasing T_p

It can be seen that the optimal values of T_p tend to increase as bandwidth increases. The overall trend of the PG for the correlation receiver is to increase with increasing T_p , whereas the PG for the energy detection receiver decreases with increasing T_p due to the quadratic interference terms.

Fig. 8 depicts the PGs as function of W_I for the correlation receiver and the energy detection receiver for $f_I = 3.325$ GHz and $T_p = \frac{2}{|f_c - f_I|} \approx 4.7$ ns. As also shown in Fig. 7, the PGs decrease with increasing bandwidth of the interferer.

The PG for the correlation receiver shows, as expected, a lower decrease with increasing W_I compared to the energy detection receiver. Energy detection receivers can suppress interference up to a bandwidth of approximately 10 MHz, whereas the linear correlation receiver can cope with up to 100 MHz bandwidth.

VI. CONCLUSIONS

This work analyzes the impact of narrowband and wideband interference on the performance of PPM energy detection receivers. The derived analytical expressions reveal the robustness of PPM energy detection to narrowband interference, which is similar to the interference suppression capability of the linear pulse correlation receiver. Furthermore, optimal values for the integration time are found, which minimize the variance of the interference part of the decision variable. In case of wideband interference, fundamental performance limits of the energy detection receiver have been derived. It has

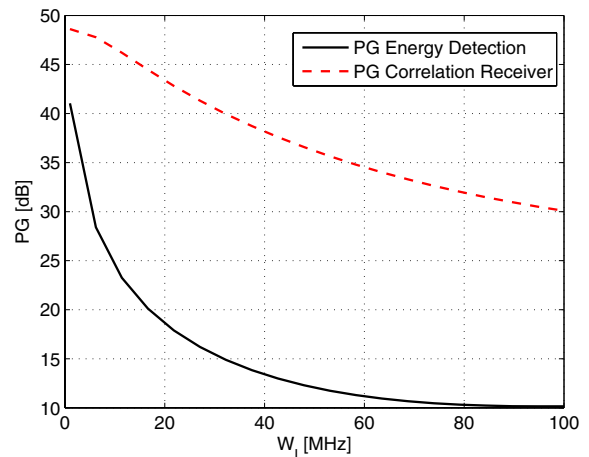


Fig. 8. Processing gains for correlation receiver and energy detection receiver for increasing W_I

been shown that the processing gain for the energy detector decreases for increasing interferer bandwidth much faster than for the correlation receiver. Significant processing gains for the energy detection receiver can only be expected for interferer bandwidths below 10 MHz.

REFERENCES

- [1] D. Porcino and W. Hirt, "Ultra-wideband radio technology: Potential and challenges ahead," *IEEE Communications Magazine*, vol. 41, no. 7, pp. 66–74, July 2003.
- [2] "Revision of part 15 of the commission's rules regarding ultra-wideband transmission systems," First Report and Order, ET Doc. 98-153, FCC 02-48, Adopted: February 14, 2002, Released: April 22, 2002, Federal Communications Commission (FCC).
- [3] "ECC decision of 24 march 2006 on the harmonised conditions for devices using ultra-wideband (UWB) technology in bands below 10.6 GHz," Electronic Communications Committee (ECC).
- [4] L. Stoica, A. Rabbachin, H. Repo, T. Tiuraniemi, and I. Oppermann, "An ultrawideband system architecture for tag based wireless sensor networks," *IEEE Transactions on Vehicular Technology*, vol. 54, no. 5, pp. 1632–1645, September 2005.
- [5] F. Troesch, C. Steiner, T. Zasowski, T. Burger, and A. Wittneben, "Hardware aware optimization of an ultra low power UWB communication system," in *IEEE International Conference on Ultra-Wideband*, Singapore, Sept. 2007, submitted.
- [6] L. Zhao and A. M. Haimovich, "Performance of ultra-wideband communications in the presence of interference," *IEEE Journal on Selected Areas in Communications*, vol. 20, no. 9, pp. 1684–1691, Dec. 2002.
- [7] M. Pausini and G. J. M. Janssen, "On the narrowband interference in UWB transmitted reference receivers," in *IEEE International Conference on Ultra-Wideband*, Zurich, CH, Sept. 2005, pp. 571–575.
- [8] T. Quek, M. Win, and D. Dardari, "UWB transmitted reference signaling schemes - part ii: narrowband interference analysis," in *IEEE International Conference on Ultra-Wideband*, Zurich, CH, Sept. 2005, pp. 593–598.
- [9] K. Witrisal and Y. Alemseged, "Narrowband interference mitigation for differential UWB systems," in *Conference Record of the Thirty-Ninth Asilomar Conference on Signals, Systems and Computers*, Oct. 2005, pp. 177–181.
- [10] D. Bukofzer, "On the squared gaussian narrowband process and its utility in the characterization of the PDF of the product of two gaussian variates," in *IEEE International Symposium on Information Theory*, June 1991, p. 73.